

FOOD & CHEMISTRY

IQGAP1, a signaling scaffold protein, as a molecular target of a small molecule inhibitor to interfere with T cell receptor-mediated integrin activation

Lin-Ying Li¹, Thi Minh Nguyet Nguyen¹, Eui Jeon Woo², Jongtae Park³, Inkyu Hwang^{1,*}

¹College of Pharmacy and Pharmaceutical Science, Chungnam National University, Daejeon 34134, Korea

²Korea Research Institute of Bioscience and Biotechnology, Daejeon 34141, Korea

³Department of Food Science and Technology, College of Agriculture, Chungnam National University, Daejeon 34134, Korea

*Corresponding author: hwanginkyu@gmail.com

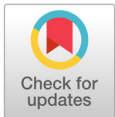
Abstract

Integrins such as lymphocyte function-associated antigen -1 (LFA-1) have an essential role in T cell immunity. Integrin activation, namely, the transition from the inactive conformation to the active one, takes place when an intracellular signal is generated by specific receptors such as T cell receptors (TCRs) and chemokine receptors in T cells. In an effort to explore the molecular mechanisms underlying the TCR-mediated LFA-1 activation, we had previously established a high-throughput cell-based assay and screened a chemical library deposited in the National Institute of Health in the United States. As a result, several hits had been isolated including HIKS-1 (Benzo[b]thiophene-3-carboxylic acid, 2-[3-[(2-carboxyphenyl) thio]-2,5-dioxo-1-pyrrolinyl]-4,5,6,7-tetrahydro-,3-ethyl ester). In an attempt to reveal the mode of action of HIKS-1, in this study, we did drug affinity responsive target stability (DARTS) assay finding that HIKS-1 interacted with the IQ motif containing GTPase activating protein 1 (IQGAP1), a 189 kDa multidomain scaffold protein critically involved in various signaling mechanisms. Furthermore, the cellular thermal shift assay (CETSA) provided compelling evidence that HIKS-1 also interacted with IQGAP1 *in vivo*. Taken together, it can be concluded that HIKS-1 interferes with the TCR-mediated LFA-1 activation by interacting with IQGAP1 and thereby disrupting the signaling pathway for LFA-1 activation.

Keywords: cellular thermal shift assay, drug affinity responsive target stability, IQ motif containing GTPase activating protein 1, lymphocyte function associated antigen-1, T cell receptor

Introduction

T cell integrins represented by lymphocyte function-associated antigen-1 (LFA-1) play essential roles in T cell immunity as both an adhesion molecule and a signaling receptor (Hogg et al., 2011;



OPEN ACCESS

Citation: Li LY, Nguyen TMN, Woo EJ, Park J, Hwang I. 2020. IQGAP1, a signaling scaffold protein, as a molecular target of a small molecule inhibitor to interfere with T cell receptor-mediated integrin activation. Korean Journal of Agricultural Science 47:361-373. <https://doi.org/10.7744/kjoas.20200026>

Received: March 16, 2020

Revised: May 15, 2020

Accepted: May 20, 2020

Copyright: © 2020 Korean Journal of Agricultural Science



This is an Open Access article distributed under the terms of the Creative Commons Attribution Non-Commercial License (<http://creativecommons.org/licenses/by-nc/4.0/>) which permits unrestricted non-commercial use, distribution, and reproduction in any medium, provided the original work is properly cited.

Verma and Kelleher, 2017). Different from other receptors, integrins in resting T cells exist in the inactive form where they are not able to interact with their ligands such as intercellular adhesion molecule-1 (ICAM-1). Transformation of LFA-1 from the inactive form to the active one is induced by a specific intracellular signal, called “Inside-out signal,” generated by specific receptors such as T cell receptor (TCR) and chemokine receptors (Abram and Lowell, 2009). The integrin activation involves many signaling molecules and dynamic rearrangement of the actin cytoskeleton and is critical not only for T cell activation but also T cell migration and execution of T cell effector functions (Walling and Kim, 2018).

Chemical genetics, the use of small molecules to perturb a biological system to explore the outcome, has emerged as a useful tool for studying a physiological mechanism (O' Connor et al., 2011). Chemical genetics approaches generally involve a high-throughput (HT) cell-based assay that not only reflects key features of the biological pathway of interest but is fit for screening a large number of chemicals in a short period of time (An and Tolliday, 2009; Ding et al., 2017). Investigating the molecular mechanism underlying TCR-mediated LFA-1 activation using the forward genetics approach, in the earlier study, we had developed a high-throughput assay with T cells isolated from 2C TCR transgenic (Tg) mice and nanometric vesicles expressing both L^d, a mouse major histocompatibility complex I (MHCI), loaded with a cognate peptide (i.e., QL9) and ICAM-1 (Kim et al., 2009a, 2009b). We also had screened a chemical library deposited in National Institute of Health (United States) in collaboration with the high-throughput flow cytometry screening center in the University of New Mexico (Hwang et al., 2009). As a result, several hits including HIKS-1 (Benzo[b]thiophene-3-carboxylic acid, 2-[3-[(2-carboxyphenyl) thio]-2,5-dioxo-1-pyrrolinyl]-4,5,6,7-tetrahydro-,3-ethyl ester) had been isolated.

A vital task faced after isolation of hits from a cell-based high-throughput screening is the identification of their target proteins in the cell (Ziegler et al., 2013). Different from hits isolated from a target-based screening, modes of action of the hits from a cell-based screening are hardly elucidated until their targets are identified. While several methods have been developed and used widely for identifying molecular targets of the hits from a cell-based screening, the target identification process is still considered a bottleneck in implementing chemical genetics studies. It has been a particularly tricky task for biologists as most target identification methods demand extensive knowledge and experience in organic synthesis for chemical modification of the hits (Schenone et al., 2013). Recently, however, a method, called “drug affinity responsive target stability (DARTS), has been developed to make it attainable to identify molecular targets of the hits without their chemical modification (Lomenick et al., 2009; Pai et al., 2015). DARTS is based on the intrinsic property of proteins that their conformational stability tends to increase when they form a complex with a specific small molecule ligand, decreasing their proteolytic susceptibilities.

In this study, we carried out DARTS to reveal a molecular target of HIKS-1. As a result, 189 kDa protein identified as IQ motif containing GTPase activating protein 1 (IQGAP1) (Hedman et al., 2015; Smith et al., 2015) was found to interact with the compound *in vitro*. We also examined the *in vivo* relevance of the finding from DARTS using cellular thermal shift assay (CETSA) (Martinez Molina et al., 2013; Martinez Molina and Nordlund, 2016) and could obtain evidence that HIKS-1 interacted with IQGAP1 inside the cell as well. Given the role of IQGAP1 in integrin activation and cell migration, those results imply that HIKS-1 is a useful tool not only as a molecular probe for investigating the action mechanism of IQGAP1 but also as a lead in developing therapeutics for treatments of immunological diseases.

Materials and Methods

Mice

2C TCR Tg mice (Sha et al., 1988) were purchased from RIKEN Bioresource Research Center (Tsukuba, Japan) and maintained in Central Animal Resource Center in the Chungnam National University (Daejeon, Korea). C57BL/6 (B6) mice were purchased from Samtako Inc. (Osan, Korea).

Antibodies and other agents

Phycoerythrin (PE)-conjugated anti-mCD80 (B7-1) (16-10A1), allophycocyanin (APC)-conjugated anti-mCD8 (53-6.7), anti-mCD11a (M17/4) were purchased from eBioscience (San Diego, USA). Anti-IQGAP1 (AF1) and anti- β -actin (C4) mAbs and horseradish peroxidase (HRP)-conjugated goat anti-mIgG Ab were purchased from Thermo Fisher (Carlsbad, USA). M-PER™ mammalian protein extraction reagent and Pierce™ BCA protein assay kit were purchased from Thermo Fisher. ECL PLUS detection kit was purchased from BioFact (Daejeon, Korea). Pronase from *Streptomyces griseus* was purchased from Sigma-Aldrich. Schneider's medium, RPMI medium and fetal bovine serum (FBS) were purchased from Thermo Fisher. QL9 (QLSPFPFDL) and P1A (LPYLGWLVF) peptides were purchased from Peptron (Daejeon, Korea).

HIKS-1 (Benzo[b]thiophene-3-carboxylic acid, 2-[3-[(2-carboxyphenyl) thio]-2,5-dioxo-1-pyrrolinyl]-4,5,6,7-tetrahydro-,3-ethyl ester) was purchased from OTAVACHemicals (Ontario, Canada).

Preparation of nanometric membrane vesicles expressing L^d MHCI, ICAM-1, and B7-1

Drosophila (Dros) S2 cells expressing L^d MHCI, mouse ICAM-1 and mouse B7-1 (CD80) were cultured in Schneider's medium containing 10% fetal bovine serum (FBS) as described. Nano-sized Dros membrane vesicles expressing L^d MHCI, ICAM-1 and B7-1 were prepared as described elsewhere (Kim et al., 2009a; Hwang et al., 2017).

T cell purification

CD8⁺ 2C Tg T cells were purified from single cell suspensions prepared from whole body lymph nodes of 2C TCR Tg mice using CD8a⁺ T Cell Isolation Kit (Miltenyi Biotech, Bergisch Gladbach, Germany).

Assay for TCR- plus LFA-1-mediated 2C T cell absorption of nanometric membrane vesicles

The membrane vesicle absorption assay was performed as described previously (Martinez Molina, 2013). Briefly, purified 2C TCR Tg T cells were cultured with QL9- or P1A-loaded Dros membrane vesicles in a 96-well plate for 90 min at 37°C. The cells were then washed once with FACS buffer (1x PBS, 2.5% horse serum, 1% BSA, 2 mM EDTA) and stained with APC-conjugated anti-CD8 plus PE-conjugated anti-B7-1 mAbs and propidium iodide (PI). After wash, the cells were analyzed with flow cytometry for the level of B7-1 expression. Flow cytometry was carried out with BD FACSCanto™ (BD Bioscience, San Jose, USA).

Drug affinity responsive target stability (DARTS) assay

DARTS assay was carried out as described by Pai et al. (2015). Briefly, the lymph node (LNs) and the thymus were harvested from the B6 mouse, and the cells were isolated from those tissues. After a couple of wash with ice-cold 1x PBS, the cells (1×10^8) were lysed with 200 μ L M-PER lysis buffer. The cell lysate was spun for 12 min at 12,000 g (4°C). After the spin, the cleared cell lysate was mixed with a one-tenth volume of 10x TNC buffer (500 mM Tris-HCl, pH 8.0, 500 mM NaCl, 100 mM CaCl_2). The cell lysate was then split into two tubes and incubated with either DMSO or HIKS-1 dissolved in DMSO for 1 hr at rt. After incubation with the compound, the cell lysate was divided into aliquots (40 μ L) and incubated with pronase for 20 - 30 min at rt. The pronase digestion was stopped by mixing the samples with 10 μ L 5x gel loading buffer (250 mM Tris-HCl, pH 6.8, 10% SDS, 500 mM β -mercaptoethanol, 0.5% bromophenol blue, 50% glycerol) and heating at 95°C for 5 min. Proteins in the pronase-treated cell lysate were then separated by SDS-polyacrylamide gel electrophoresis (PAGE) and analyzed by either Coomassie Blue staining or Western blot.

LC-MS/MS for protein identification

Protein LC-MS/MS analysis was carried out in Proteomtech Inc. (Seoul, Korea). Briefly, after completing DARTS assay as described above, proteins in the pronase-treated cell lysate were separated by SDS-PAGE and stained with Coomassie Blue. Then, a small piece of gel block containing ~ 190 kDa protein was excised out. Proteins in the gel block were digested with trypsin and the peptides were extracted as described by Bahk et al. (2004). The extracted peptides were subjected to a desalting process using reverse-phase column chromatography (Gobom et al., 1999).

LC-MS/MS analysis was performed through nano ACQUITY UPLC and LTQ-orbitrap-mass spectrometer (Thermo Electron, San Jose, USA). The column used BEH C18 1.7 μm , 100 $\mu\text{m} \times 100$ mm column (Waters, Milford, MA, USA). The mobile phase A for the LC separation was 0.1% formic acid in deionized water and the mobile phase B was 0.1% formic acid in acetonitrile. The chromatography gradient was set up to give a linear increase from 10% B to 40% B for 21 min, from 40% B to 95% B for 7 min, and from 90% B to 10% B for 10 min. The flow rate was $0.5 \mu\text{L} \cdot \text{min}^{-1}$. For tandem mass spectrometry, mass spectra were acquired using data-dependent acquisition with full mass scan (300 - 2000 m/z) followed by MS/MS scans. Each MS/MS scan acquired was an average of one microscans on the LTQ. The temperature of the ion transfer tube was controlled at 160°C and the spray was 1.5 - 2.0 kV. The normalized collision energy was set at 35% for MS/MS. The individual spectra from MS/MS were processed using the SEQUEST software (Thermo Quest, San Jose, USA) and the generated peak lists were used to query in house database using the MASCOT program (Matrix Science Ltd., London, UK). We set the modifications of Carbamidomethyl (C), Deamidated (NQ), Oxidation (M) for MS analysis and tolerance of peptide mass was 10 ppm. MS/MS ion mass tolerance was 0.8 Da, allowance of missed cleavage was 2, and charge states (+2, +3) were taken into account for data analysis. We took only significant hits as defined by MASCOT probability analysis.

Western blot analysis

Western blot analyses were performed as described previously (Hwang et al., 2017). Briefly, proteins (15 mg) in the cell lysates were separated by SDS-PAGE and electrically transferred to PVDF membrane (ATTA, AE-6667-P) followed by treatment with the blocking buffer (20 mM Tris-HCl, pH 7.2, 150 mM NaCl, 0.05% Tween 20, 10% non-fat milk). The membrane was then incubated with either anti-IQGAP1 or β -actin mAb. After extensive wash, the membrane was incubated with HRP-conjugated goat anti-mouse IgG. After wash, the membrane was treated with ECL PLUS detection solution, and the intensities of chemiluminescent bands were quantitatively measured with ImageQuantTM LAS 400 biomolecular imager (GE Healthcare).

CETSA assay

CETSA assay was carried out as described by Jafari et al. (2014). Briefly, cells were isolated from the whole body LNs and the thymus harvested from the B6 mouse. After a couple of wash, the cells were cultured with either DMSO or HIKS-1 in DMSO for half an hour at 37°C in a humidified CO₂ incubator. After incubation, the cells were washed with ice-cold 1x PBS and resuspended in 600 μ L ice-cold 1x PBS. The cells were then divided into aliquots (100 μ L) and spun down for 2 min at 120 g (4°C). After centrifugation, 80 μ L of supernatant was carefully removed, and the cells in the pellet were resuspended in the remaining buffer. The resulting cell suspensions were treated with heat for 3 min at several different temperatures followed by incubation for 3 min at rt. Thereafter, the cells were lysed by repeated freezing and thawing. The cell lysates were then supplemented with 30 μ L 1x PBS and spun down to separate denatured (precipitated) proteins. After the spin, the supernatants (44 μ L) were taken and mixed with the gel loading buffer. Proteins in the mixtures were separated by SDS-PAGE and the levels of IQGAP1 were analyzed by Western blot.

Results

Inhibition by HIKS-1 of 2C T cell absorption of nanometric membrane vesicles expressing cognate pMHC (L^d/QL9) plus ICAM-1 and B7-1

In the earlier study, we had screened a chemical library deposited in NIH with the HT flow cytometry assay in collaboration with the HT flow cytometry screening center in The University of New Mexico; the summary report had been archived in National Center for Biotechnology Information (NCBI) website (Hwang et al., 2009). Several hits including HIKS-1 (Fig. 1A) had been isolated as a result of the high-throughput screening (HTS). We chose the HIKS-1 for further study as it showed the strongest activity for the inhibition of the membrane vesicle absorption by 2C TCR Tg T cells with the least cytotoxicity among the hits; IC₅₀ for HIKS-1 was determined at 8 μ M (Fig. 1C), and it showed no cytotoxicity against 2C TCT Tg T cells even at 25 μ M (Fig. 1D). As having been reported previously (Kim et al., 2009a), it was assured that both 2C TCR-L^d/QL9 and LFA-1-ICAM-1 interactions were mandatory for the membrane vesicle absorption by 2C TCR Tg T cells (Fig. 1B).

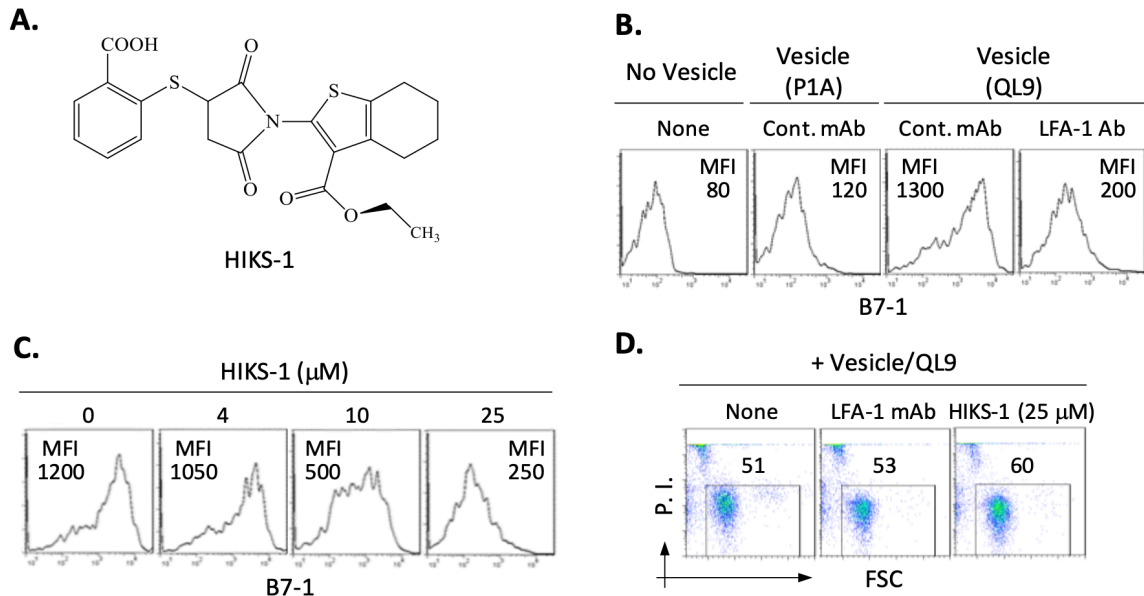


Fig. 1. Inhibition by HIKS-1 of T cell receptor (TCR)-plus lymphocyte function-associated antigen-1 (LFA-1)-mediated 2C TCR Tg T cell absorption of Dros membrane vesicles. (A) The chemical structure of HIKS-1 is shown. (B) Purified 2C TCR Tg T cells were cultured with P1A- or QL9-loaded Dros membrane vesicles expressing L^d MHCI, ICAM-1 and B7-1 for 90 min at 37°C in the presence or absence of anti-LFA-1 alpha chain (αL) mAb (5 μg·mL⁻¹) as indicated. After culture, cells were stained with APC-conjugated anti-CD8 plus PE-conjugated anti-B7-1 mAbs and PI. Histograms show the levels of Dros membrane vesicle-derived B7-1 on the surface of live CD8⁺ T cells. Mean fluorescence intensities (MFIs) of histograms calculated using FlowJo software are shown inside the plots. Note that both P1A and QL9 peptides form complexes with L^d, but only L^d/QL9 complex interacts with 2C TCR. (C) Purified 2C TCR Tg T cells pre-treated with HIKS-1 for half an hour at the concentrations indicated were cultured with QL9-loaded Dros membrane vesicles. After culture, the cells were stained with the mAbs and analyzed with flow cytometry as in (A). (D) The cytotoxicity of HIKS-1 was determined with the ratio of PI-excluding (viable) 2C TCR Tg T cells after the membrane vesicles absorption assay. No decrease in the viability of the cells was observed after culture with either anti-LFA-1 mAb (5 μg·mL⁻¹) or HIKS-1 (25 μM).

Selecting a ~190 kDa protein as a putative molecular target of HIKS-1

Searching for a molecular target of HIKS-1 in T cells, we carried out DARTS with the cells isolated from the LNs and the thymus. Coomassie Blue staining of the proteins digested with pronase in the presence and the absence of HIKS-1 (1 mM), respectively, showed a noticeable difference in the intensities of the protein band with molecular weight (MW) of approximately 190 kDa, suggesting that HIKS-1 protected the ~190 kDa protein from pronase digestion (Fig. 2A). The dose effect of HIKS-1 on digestion of the ~190 kDa protein by pronase was also observed; thus, the levels of the protein remaining in the solution after pronase treatment increased as the concentrations of HIKS-1 increased (Fig. 2B).

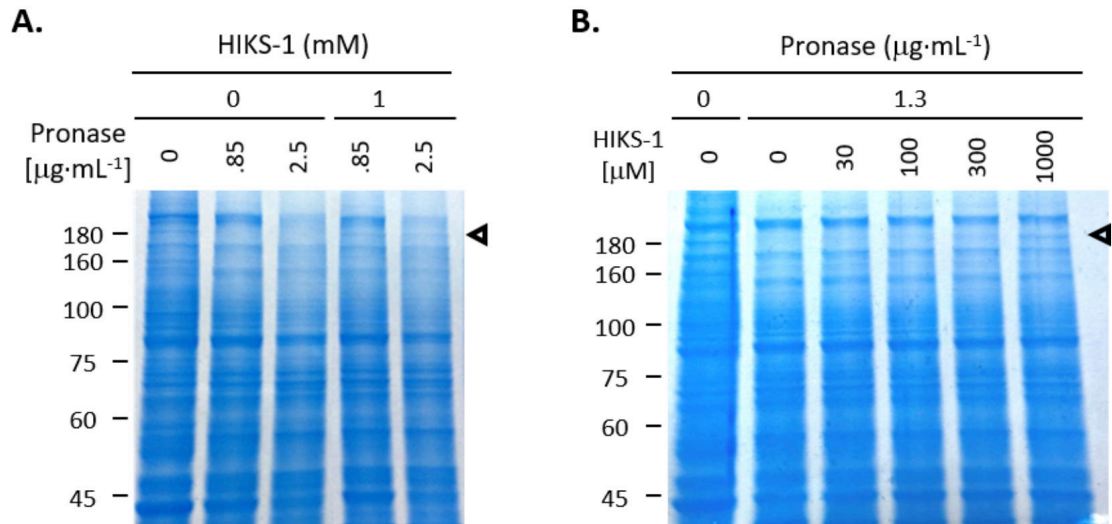


Fig. 2. Selecting a ~ 190 kDa protein as a putative molecular target of HIKS-1 via drug affinity responsive target stability (DARTS). (A) DARTS was performed with varying concentrations (0, 0.85, 2.5 $\mu\text{g}\cdot\text{mL}^{-1}$) of pronase in the presence (1 mM in DMSO) or absence (only DMSO) of HIKS-1 as indicated. (B) DARTS was carried out with increasing concentrations of HIKS-1 with (1.3 $\mu\text{g}\cdot\text{mL}^{-1}$) or without pronase as indicated. In both (A) and (B), band intensities of the ~ 190 kDa protein marked by an arrow were found stronger when pronase digestion was done in the presence of HIKS-1. Further, the band intensity increased progressively as the concentration of HIKS-1 was raised, as shown in (B).

Identifying IQGAP1 as a molecular target of HIKS-1

Disclosing the identity of the ~ 190 kDa protein, we repeated DARTS with the cell lysate prepared from the cells isolated from the LNs and the thymus, and a piece of polyacrylamide gel containing the ~ 190 kDa protein band was excised out. Proteins in the gel slice were then digested with trypsin, and the resulting peptides were subjected to mass spectrometry (LC-MS/MS). Data from the mass spectroscopy showed that the protein called “IQ motif containing GTPase activating protein 1 (IQGAP1)” whose molecular weight is 189 kDa (Hedman et al., 2015; Smith et al., 2015) received the highest score among the proteins found in the gel slice; total of 20 IQGAP1-derived peptides were identified by the mass spectroscopy (Fig. 3).

Verifying that HIKS-1 protected IQGAP1 from pronase digestion, we performed Western blot analysis with anti-IQGAP1 mAb following DARTS. Of note, the levels of intact IQGAP1 remaining after pronase digestion were markedly higher when it was carried out in the presence of HIKS-1 than when done in the absence of it (Fig. 4A). The dose effect of HIKS-1 was also evident; thus, the levels of IQGAP1 detected in the Western blot analysis increased progressively as the concentrations of HIKS-1 in the pronase reaction mixtures increased (Fig. 4B). Intriguingly, it was found that a protein band with the molecular weight of approximately ~ 80 kDa newly appeared when IQGAP1 was digested by pronase (Fig. 4). We postulated that the ~ 80 kDa protein was a truncated form of IQGAP1 resulting from proteolytic cleavage of full-length IQGAP1. Accordingly, it was noticed the intensities of the ~ 80 kDa protein band were inversely correlated with those of full-length IQGAP1.

gi 7331254 Mass: 189636 Score: 494 Matches: 20(16) Sequences: 18(15) emPAI: 0.44 IQ motif containing GTPase activating protein 1 [Mus musculus]										
Query	Observed	Mr(expt)	Mr(calc)	ppm	Miss	Score	Expect	Rank	Unique	Peptide
100	383.2108	764.4070	764.4068	0.27	0	46	0.00051	1	U	R.NGVYLA.K
190	414.2709	826.5272	826.5276	-0.47	0	27	0.023	1	U	R.LMDVIR.F
390	455.7368	909.4590	909.4596	-0.63	0	31	0.041	1	U	K.LGNFFSPK.V
456	475.7451	949.4756	949.4757	-0.01	0	29	0.063	1	U	K.TDPVDYK.S
481	484.7556	967.4966	967.4975	-0.83	0	27	0.072	1	U	R.DHINDIK.I
526	492.3215	982.6284	982.6287	-0.30	1	39	0.00045	1	U	K.RLIVDVIR.F
694	518.7870	1035.5594	1035.5601	-0.59	0	71	2.5e-006	1	U	R.VAADTFTALK.N
799	536.7977	1071.5808	1071.5812	-0.32	0	63	7.5e-005	1	U	K.LTELGTVDPK.N
864	364.8696	1091.5870	1091.5876	-0.58	1	27	0.1	1	U	R.YKATGLHFR.H
866	547.2455	1092.4764	1092.4757	0.68	0	51	0.0003	1	U	R.LTAEEMDER.R
1352	600.8453	1199.6760	1199.6761	-0.08	1	34	0.012	1	U	K.KLTELGTVDPK.N
2165	630.3605	1258.7064	1258.7067	-0.21	1	45	0.00088	1	U	K.MREEVITLIR.S
2166	420.5761	1258.7065	1258.7067	-0.19	1	(27)	0.055	1	U	K.MREEVITLIR.S
2750	669.3237	1336.6328	1336.6333	-0.34	0	76	1e-006	1	U	R.ALESGDMTTVWK.Q
2832	677.3206	1352.6266	1352.6282	-1.16	0	(49)	0.00063	1	U	R.ALESGDMTTVWK.Q + Oxidation (M)
3753	766.8666	1531.7186	1531.7195	-0.53	0	55	0.00015	1	U	K.IFYPETTDIYDR.K
4207	830.9141	1659.8136	1659.8144	-0.47	1	61	3.7e-005	1	U	K.IFYPETTDIYDR.N
4875	946.4732	1890.9318	1890.9323	-0.25	0	33	0.021	1	U	R.FALGISAINAEVDSGDVGR.T
4993	648.3176	1941.9310	1941.9320	-0.51	1	44	0.0016	1	U	K.DSLHEKFPDAGEDELLK.I
7734	1070.1764	3207.5074	3207.5104	-0.94	1	38	0.0054	1	U	R.WMEACLGEDLPPTTELEEGLRNGVYLA.K + Oxidation (M)

Fig. 3. LC-MS/MS analysis to unveil the sequence identity of the ~ 190 kDa protein. Following drug affinity responsive target stability (DARTS), a small piece of acrylamide gel containing the ~ 190 kDa protein was excised out. Proteins in the gel block were then digested with trypsin, and the peptides were extracted (see the experimental for details). The extracted peptides were then subjected to LC-MS/MS analysis to determine their amino acid sequences. The results demonstrated that the ~ 190 kDa protein is most likely the protein called IQ motif containing GTPase activating protein 1 (IQGAP1). Twenty different IQGAP1-derived peptides were identified by the mass analysis, as shown in this figure.

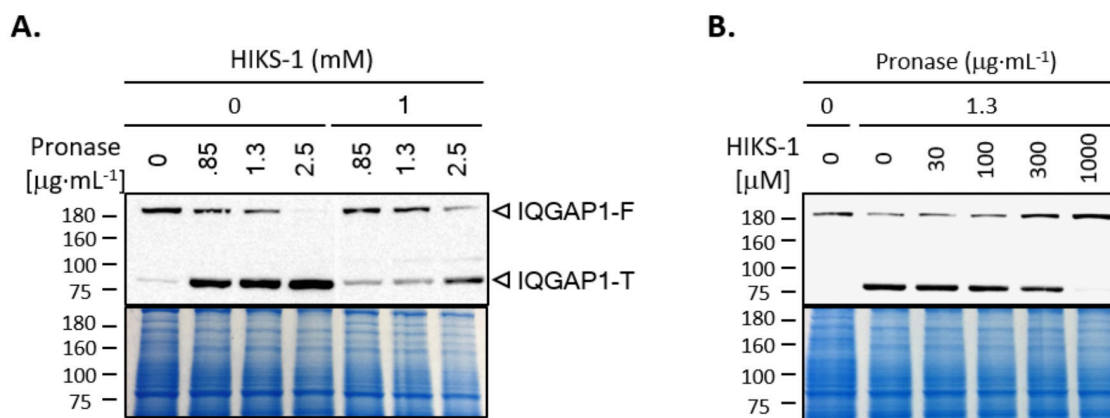


Fig. 4. Verifying with Western blot analysis that IQ motif containing GTPase activating protein 1 (IQGAP1) is the protein protected from pronase by HIKS-1. (A) Following drug affinity responsive target stability (DARTS) with varying concentration of pronase in the presence (1 mM) or the absence of HIKS-1 as indicated, proteins in the cell lysates were separated by SDS-PAGE for Western blot analysis with anti-IQGAP1 mAb and Coomassie Blue staining, respectively. (B) Following DARTS with increasing concentrations of HIKS-1 as indicated, proteins in the cell lysates were separated by SDS-PAGE for Western blot analysis with anti-IQGAP1 mAb and Coomassie Blue staining, respectively. Note that the new Western band (~ 80 kDa) appeared after pronase treatment.

Interaction of HIKS-1 with IQGAP1 *in vivo*

While the results from DARTS strongly indicated that HIKS-1 interacted with IQGAP1 *in vitro* to promote its conformational stability, it had yet to be addressed whether HIKS-1 interacted with the protein inside the cell as well. Examining whether HIKS-1 interacted with IQGAP1 *in vivo*, we employed CETSA, the method used for investigating the interaction of a small molecule with its putative target protein *in vivo* based on the change in thermal stability of the protein after forming a complex with the small molecule.

CETSA was carried out with the cells isolated from the LNs and the thymus. Expectedly, the level of soluble IQGAP1 decreased steadily in the cells with no HIKS-1 treatment as incubation temperature rose. Surprisingly, when the cells were incubated with the compound, the level of intact IQGAP1 remaining after the heat treatments decreased more precipitously (Fig. 5A). The dose effect of HIKS-1 on the change in thermal stability of IQGAP1 was also found apparent; thus, the levels of soluble IQGAP1 remaining in the cytosol decreased progressively as the concentration of HIKS-1 increased (Fig. 5B and Fig. 5C). These results suggested that HIKS-1 also interacted with IQGAP1 *in vivo*, but the interaction resulted in a decrease in thermal stability of IQGAP1 (Fig. 6).

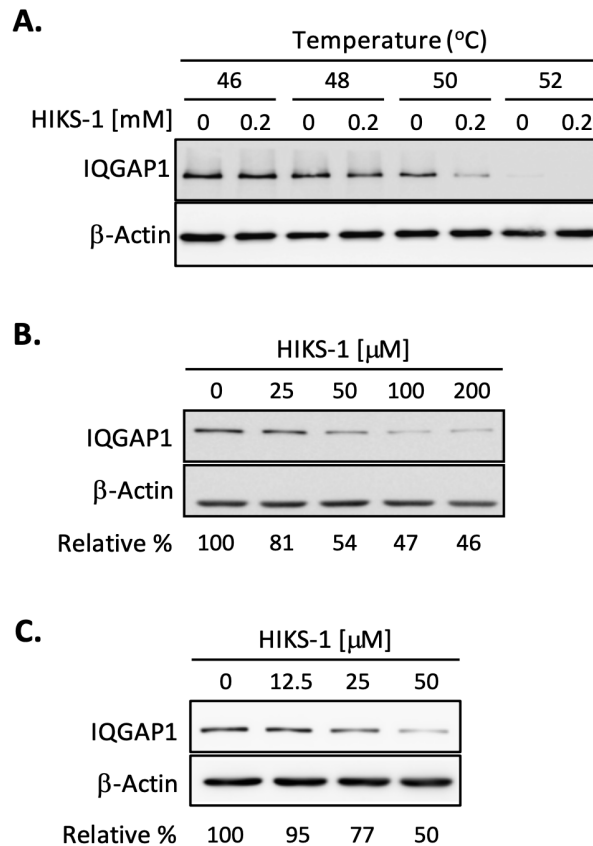


Fig. 5. Verifying the interaction between HIKS-1 and IQ motif containing GTPase activating protein 1 (IQGAP1) *in vivo* with cellular thermal shift assay (CETSA). (A) Cells isolated from the lymph node (LNs) and the thymus of the B6 mice were incubated at different temperatures in the presence (0.2 mM) or absence of HIKS-1 as indicated. Denatured (insoluble) proteins were then removed by centrifugation, and intact (soluble) proteins were subjected to Western blot analysis with anti-IQGAP1 mAb. (B) CETSA was carried out at 50°C with varying concentrations of HIKS-1 as indicated. (C) CETSA was carried out as in (B) with lower concentrations of HIKS-1 as indicated. Band intensities of IQGAP1 relative to those of β-actin were determined first, and the ratios of the relative intensities to that of 0 μM HIKS-1 were calculated, respectively. The ratios are denoted as relative % (B and C).

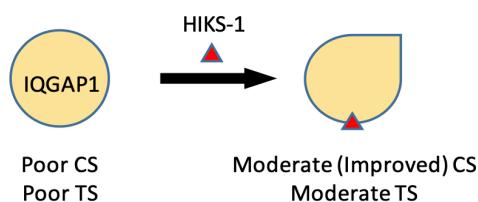
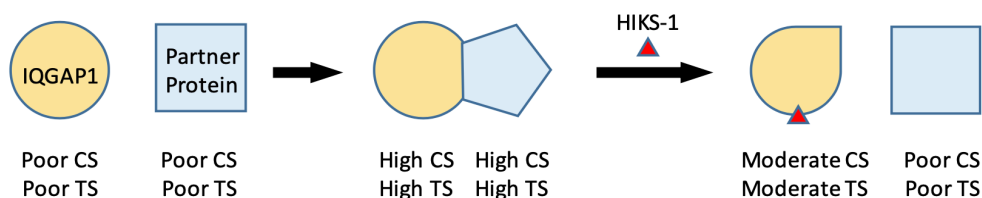
A. Increase in the thermal stability of a protein by its small molecule ligand**B. Decrease in the relative thermal stability of a protein by its small molecule ligand**

Fig. 6. A hypothesis proposed to explain the decrease in thermal stability of IQ motif containing GTPase activating protein 1 (IQGAP1) following interaction with HIKS-1 *in vivo*. (A) The structure of a protein tends to be stabilized, increasing its thermal stability (TS) when it forms a complex with a specific small molecule ligand. (B) Similarly, the structure of a protein is also stabilized when it creates a complex with other protein(s). The extent of conformational stabilization (CS) by the protein-protein interaction may exceed that by the protein-small molecule interaction. Thus, in the case that a large portion of a protein is already engaged with other protein (s) to form a protein-protein complex and that a small molecule interacts with the protein to interfere with the formation of the protein-protein complex, the small molecule-protein interaction may result in decrease in overall thermal stability of the protein.

Discussion

The target identification is considered the most time-consuming and a rate-limiting step in chemical genetics approach. It has been particularly troublesome for biologists as traditional target identification methods require organic modifications of molecules of interest. In recent years, however, several organic synthesis-free methods have been developed, making the target identification possible without extensive knowledge and experiences in organic synthesis. This study proved the effectiveness of DARTS as an organic synthesis-free target identification method.

IQGAP1 is a scaffold protein with several functional domains. N-terminal calponin homology domain (CHD) is known to be responsible for linking IQGAP1 to the actin cytoskeleton (Sjoblom et al., 2008). GAP-related domain (GRD) in the C-terminal is known to be involved in the interaction with small GTP-binding proteins such as Rac and Cdc42 (Mack and Georgiou, 2014). IQ motif domain in the middle part of the protein is necessary for interaction with calmodulin (a calcium-binding protein) (Pathmanathan et al., 2011). Given the importance of the actin cytoskeleton, small GTP-binding proteins and calcium in integrin activation (Abram and Lowell, 2009; Hogg et al., 2011; Verma and Kelleher, 2017), our results imply that HIKS-1 inhibits 2C TCR Tg T cell absorption of QL9-loaded Dros membrane vesicles by compromising the function of IQGAP1 in “Inside-out-signaling” for integrin activation. Indeed, a few studies have demonstrated the critical role of IQGAP1 in integrin activation even though its role in TCR-mediated LFA-1 activation has not been reported yet (Choi et al., 2013; Jacquemet et al., 2013).

The result of CETSA is somewhat puzzling as it is more common that the thermal stability of a protein increases when it forms a complex with a small molecule ligand. Thus, under the premise that HIKS-1 interacted with IQGAP1 inside the cell, it was expected that the thermal stability of cellular IQGAP1 could be promoted when the cells were incubated with HIKS-1. The result from CETSA turned out opposite to the expectation. While more studies must be done to interpret the result accurately, the CETSA result suggests that the conformation of IQGAP1 be converted to a less stable form when it interacts with HIKS-1 inside the cell. Indeed, there are a few reports that thermal stabilities of proteins can be lowered after interaction with their specific small molecule ligand (Martinez Molina, 2013; Jafari, 2014). Diminution in protein thermal stability after interaction with a small molecule ligand is observed more often in the proteins constantly forming complexes with other proteins inside the cell. Based on the information from the literature, we propose a hypothesis to explain the CETSA result as follow.

It is supposed that thermal stability of IQGAP1 escalates when it forms a complex with other proteins (e.g., actin cytoskeleton, small GTP-binding proteins, and calmodulin, etc.) as such interactions may stabilize the conformation of IQGAP1 (Fig. 6). Based on that supposition, it is proposed that overall thermal stability of IQGAP1 may decline when HIKS-1 interacts with IQGAP1 to interfere with the formation of a multi-protein complex centered by IQGAP1. More studies are warranted to test the hypothesis.

Expression of full-length recombinant IQGAP1 has not been reported yet. According to the literature, even expressing the truncated forms of IQGAP1, particularly ones that contain C-terminal half of the protein, in a soluble form seems very challenging. Due to the difficulty in expressing recombinant IQGAP1, the information about its structural properties is quite limited, making it difficult to investigate the mode of interaction between HIKS-1 and IQGAP1. Still, expression of several short IQGAP1 fragments has been reported by others (Pelikan-Conchaudron et al., 2011), and we are examining whether HIKS-1 interacts with one of those fragments using surface plasmon resonance (SPR)(Hinman et al., 2018) and isothermal titration calorimetry (ITC) technologies (Freyer and Lewis, 2008).

Conclusion

In use of the novel high-throughput flow cytometry assay, we screened a large size chemical library deposited in NIH in collaboration with the New Mexico Molecular Screening Center (NMMLSC). As a result, a small molecule designated as HIKS-1 was isolated as a hit to inhibit TCR-mediated LFA-1 activation and thus overall T cell activation process. Further study revealed that HIKS-1 interacted with IQGAP-1 that has multiple functional domains critically involved in integrin activation and immune cell function.

Acknowledgments

We thank Lehong Son and Eunju Lee at the College of Pharmacy and Pharmaceutical Science in the Chungnam National University for their assistance and supports. We also thank researchers in Proteomtech Inc. (Seoul, Korea) for LC-MS/MS analysis and identification of IQGAP1. This work was supported by CNU Research Grant (2017-1795-01). L.-Y. L. and T.M.N.N. were supported by BK21Plus program by the National Research Foundation of Korea.

Authors Information

Lin-Ying Li, Chungnam National University, College of Pharmacy, Graduate student

Thi Minh Nguyet Nguyen, Chungnam National University, College of Pharmacy, Graduate Student

Eui Jeon Woo, KRIBB, Principal Research Scientist

Jongtae Park, Chungnam National University, College of Agriculture, Professor

Inkyu Hwang, Chungnam National University, College of Pharmacy, Professor

References

- Abram CL, Lowell CA. 2009. The ins and outs of leukocyte integrin signaling. *Annual Review of Immunology* 27:339-362.
- An WF, Tolliday NJ. 2009. Introduction: Cell-based assays for high-throughput screening. *Methods in Molecular Biology* 486:1-12.
- Bahk YY, Kim SA, Kim JS, Euh HJ, Bai GH, Cho SN, Kim YS. 2004. Antigens secreted from *Mycobacterium tuberculosis*: identification by proteomics approach and test for diagnostic marker. *Proteomics* 4:3299-3307.
- Choi S, Thapa N, Hedman AC, Li Z, Sacks DB, Anderson RA. 2013. IQGAP1 is a novel phosphatidylinositol 4,5 bisphosphate effector in regulation of directional cell migration. *The Embo Journal* 32:2617-2630.
- Ding M, Kaspersson K, Murray D, Bardelle C. 2017. High-throughput flow cytometry for drug discovery: Principles, applications, and case studies. *Drug Discovery Today* 22:1844-1850.
- Freyer MW, Lewis EA. 2008. Isothermal titration calorimetry: Experimental design, data analysis, and probing macromolecule/ligand binding and kinetic interactions. *Methods in Cell Biology* 84:79-113.
- Gobom J, Nordhoff E, Mirgorodskaya E, Ekman R, Roepstorff P. 1999. Sample purification and preparation technique based on nano-scale reversed-phase columns for the sensitive analysis of complex peptide mixtures by matrix-assisted laser desorption/ionization mass spectrometry. *Journal of Mass Spectrometry* 34:105-116.
- Hedman AC, Smith JM, Sacks DB. 2015. The biology of IQGAP proteins: Beyond the cytoskeleton. *EMBO Reports* 16:427-446.
- Hinman SS, McKeating KS, Cheng Q. 2018. Surface plasmon resonance: Material and interface design for universal accessibility 90:19-39.
- Hogg N, Patzak I, Willenbrock F. 2011. The insider's guide to leukocyte integrin signalling and function. *Nature Reviews Immunology* 11:416-426.
- Hwang IHM, Hu C, Waller A, Carter M, Wu Y, Sklar L. 2009. Summary report of screening for developing T cell immune modulators. Accessed in on 10 June 2019.
- Hwang I, Kim K, Choi S, Lomunova M. 2017. Potentiation of T cell stimulatory activity by chemical fixation of a weak peptide-MHC complex. *Molecules and Cells* 40:24-36.
- Jacquemet G, Morgan MR, Byron A, Humphries JD, Choi CK, Chen CS, Caswell PT, Humphries MJ. 2013. Rac1 is deactivated at integrin activation sites through an IQGAP1-filamin-A-RacGAP1 pathway. *Journal of Cell Science* 126:4121-4135.
- Jafari R, Almqvist H, Axelsson H, Ignatushchenko M, Lundback T, Nordlund P, Martinez Molina D. 2014. The cellular thermal shift assay for evaluating drug target interactions in cells. *Nature Protocols* 9:2100-2122.
- Kim K, Wang L, Hwang I. 2009a. Acute inhibition of selected membrane-proximal mouse T cell receptor signaling by mitochondrial antagonists. *PLoS One* 4:e7738.
- Kim K, Wang L, Hwang I. 2009b. A novel flow cytometric high throughput assay for a systematic study on molecular mechanisms underlying T cell receptor-mediated integrin activation. *PLoS One* 4:e6044.

- Lomenick B, Hao R, Jonai N, Chin RM, Aghajan M, Warburton S, Wang J, Wu RP, Gomez F, Loo JA, Wohlschlegel JA, Vondriska TM, Pelletier J, Herschman HR, Clardy J, Clarke CF, Huang J. 2009. Target identification using drug affinity responsive target stability (DARTS). *Proceedings of National Academy of Sciences of USA* 106:21984-21989.
- Mack NA, Georgiou M. 2014. The interdependence of the Rho GTPases and apicobasal cell polarity. *Small GTPases* 5:10.
- Martinez Molina D, Jafari R, Ignatushchenko M, Seki T, Larsson EA, Dan C, Sreekumar L, Cao Y, Nordlund P. 2013. Monitoring drug target engagement in cells and tissues using the cellular thermal shift assay. *Science* 341:84-87.
- Martinez Molina D, Nordlund P. 2016. The cellular thermal shift assay: A novel biophysical assay for in situ drug target engagement and mechanistic biomarker studies. *Annual Review of Pharmacology and Toxicology* 56:141-161.
- O' Connor CJ, Laraia L, Spring DR. 2011. Chemical genetics. *Chemical Society Reviews* 40:4332-4345.
- Pai MY, Lomenick B, Hwang H, Schiestl R, McBride W, Loo JA, Huang J. 2015. Drug affinity responsive target stability (DARTS) for small-molecule target identification. *Methods in Molecular Biology* 1263:287-298.
- Pathmanathan S, Hamilton E, Atcheson E, Timson DJ. 2011. The interaction of IQGAPs with calmodulin-like proteins. *Biochemical Society Transactions* 39:694-699.
- Pelikan-Conchaudron A, Le Clainche C, Didry D, Carlier MF. 2011. The IQGAP1 protein is a calmodulin-regulated barbed end capper of actin filaments: Possible implications in its function in cell migration. *Journal of Biological Chemistry* 286:35119-35128.
- Schenone M, Dancik V, Wagner BK, Clemons PA. 2013. Target identification and mechanism of action in chemical biology and drug discovery. *Nature Chemical Biology* 9:232-240.
- Sha WC, Nelson CA, Newberry RD, Kranz DM, Russell JH, Loh DY. 1988. Selective expression of an antigen receptor on CD8-bearing T lymphocytes in transgenic mice. *Nature* 335:271-274.
- Sjoblom B, Ylanne J, Djinojic-Carugo K. 2008. Novel structural insights into F-actin-binding and novel functions of calponin homology domains. *Current Opinion Structural Biology* 18:702-708.
- Smith JM, Hedman AC, Sacks DB. 2015. IQGAPs choreograph cellular signaling from the membrane to the nucleus. *Trends in Cell Biology* 25:171-184.
- Verma NK, Kelleher D. 2017. Not just an adhesion molecule: LFA-1 contact tunes the T lymphocyte program. *The Journal of Immunology* 199:1213-1221.
- Walling BL, Kim M. 2018. LFA-1 in T cell migration and differentiation. *Frontiers in Immunology* 9:952.
- Ziegler S, Pries V, Hedberg C, Waldmann H. 2013. Target identification for small bioactive molecules: Finding the needle in the haystack. *Angewandte Chemie International Edition* 52:2744-2792.